# Molecular architecture of $G\alpha_o$ and the structural basis for RGS16-mediated deactivation

Kevin C. Slep*†, Michele A. Kercher‡§, Thomas Wieland¶‖, Ching-Kang Chen¶, Melvin I. Simon¶**, and Paul B. Sigler‡§††

*Department of Biology, University of North Carolina, Chapel Hill, NC 27599; ‡Department of Molecular Biophysics and Biochemistry, and §Howard Hughes Medical Institute, Yale University, New Haven, CT 06511; and ¶Division of Biology, California Institute of Technology, Mail Code 147-75, Pasadena, CA 91125

Contributed by Melvin I. Simon, February 16, 2008 (sent for review December 18, 2007)

**Heterotrimeric G proteins relay extracellular cues from heptahelical transmembrane receptors to downstream effector molecules. Composed of an $\alpha$ subunit with intrinsic GTPase activity and a $\beta\gamma$ heterodimer, the trimeric complex dissociates upon receptor-mediated nucleotide exchange on the $\alpha$ subunit, enabling each component to engage downstream effector targets for either activation or inhibition as dictated in a particular pathway. To mitigate excessive effector engagement and concomitant signal transmission, the G$\alpha$ subunit's intrinsic activation timer (the rate of GTP hydrolysis) is regulated spatially and temporally by a class of GTPase accelerating proteins (GAPs) known as the regulator of G protein signaling (RGS) family. The array of G protein-coupled receptors, G$\alpha$ subunits, RGS proteins and downstream effectors in mammalian systems is vast. Understanding the molecular determinants of specificity is critical for a comprehensive mapping of the G protein system. Here, we present the 2.9 Å crystal structure of the enigmatic, neuronal G protein $G\alpha_o$ in the GTP hydrolytic transition state, complexed with RGS16. Comparison with the 1.89 Å structure of apo-RGS16, also presented here, reveals plasticity upon $G\alpha_o$ binding, the determinants for GAP activity, and the structurally unique features of $G\alpha_o$ that likely distinguish it physiologically from other members of the larger $G\alpha_i$ family, affording insight to receptor, GAP and effector specificity.**

G protein | GAP | RGS

Many extracellular cues ranging from photons to neurotransmitters are detected with high specificity by G protein-coupled receptors that in turn elicit an intracellular response by promoting GTP exchange on the $\alpha$ subunit of a heterotrimeric G protein. The heterotrimeric G protein, composed of an $\alpha$ subunit exhibiting endogenous GTPase activity and a heterodimeric $\beta\gamma$ subunit, dissociates, enabling each component to activate downstream effectors until GTP is hydrolyzed on the $\alpha$ subunit and the heterotrimeric complex reforms. The $\alpha$ subunit's endogenous GTP hydrolysis rate is relatively slow, therefore the cell uses GTPase accelerating proteins (GAPs) to increase the rate to suit the time scale and magnitude needed for a specific physiological response.

The regulators of G protein signaling (RGS) proteins are a class of heterotrimeric G protein GAP first identified in *Saccharomyces cerevisiae* (Sst2) and *Caenorhabditis elegans* (Egl10) (1, 2). Studies, both biochemical and structural, have shown an overall preference for RGS domains to bind G$\alpha$ subunits in their transition state (mimicked by the analog GDP·$AlF_4^-$) and to accelerate GTPase activity by stabilizing the transition state of hydrolysis, thereby optimizing the endogenous GTPase activity of the G$\alpha$ subunit without directly contributing to the hydrolytic mechanism (3–5). RGS proteins serve to quench the G protein signal temporally and spatially, either independently, or coupled (*in cis* or *in trans*) to an effector (6, 7). Thirty-seven RGS proteins have been identified in the human genome, cataloged into eight subfamilies based on the protein family the RGS domain resides delineated as RGS subfamilies R4, R7, R12, RZ, and RhoGEF RGS (rgRGS); G protein-coupled receptor kinases (GRKs); sorting nexins; and Axin (8–10). Each member displays a unique expression and localization pattern (11). With the number of RGS proteins greatly exceeding the number of G$\alpha$ subunits, RGS proteins are likely to be finely tuned, titrated, and localized to regulate specific signaling pathways within a G$\alpha$ subunit's repertoire of effector targets. To mediate the specificity and fidelity requisite for accurate signal transmission, the G$\alpha$ subunit and its binding partners (GPCR, G$\beta\gamma$, RGS, and effector) must have specific reciprocating molecular determinants to minimize the convergence of independent signaling pathways. Thus, a comprehensive understanding of the molecular basis for G$\alpha$ engagement with its activators, regulators, and effectors is critical for elucidating specificity determinants. RGS subfamilies pair with distinct cognate G$\alpha$ substrates via unique stereochemical binding determinants. The RGS subfamilies R4, R7, and R12 engage $G\alpha_{i/o}$ (3, 12, 13); the R4 subfamily also engages $G\alpha_q$ (14); the rgRGS subfamily engages $G\alpha_{12/13}$ (15); and the RZ subfamily engages $G\alpha_z$ and $G\alpha_i$ (3, 16, 17). It is noted that G$\alpha$–RGS interaction modes observed in R4, R7 and R12 (5, 7) [see accompanying article by Soundararajan *et al.* (18)] contrast with the unique interlocking geometry observed between p115RhoGEF rgRGS and the $G\alpha_{13/i1}$ chimera (19) and the effector-like binding mode observed between GRK2 and $G\alpha_q$ (20).

$G\alpha_o$ is a member of the $G\alpha_i$ family, which includes $G\alpha_{i1\text{-}3}$ and $G\alpha_t$. Although $G\alpha_o$ is the most abundant G$\alpha$ subunit in the human brain, little is known about the pathways it is involved in, in stark contrast to our understanding of $G\alpha_{i1\text{-}3}$ and $G\alpha_t$. Much of the work on $G\alpha_o$ to date has implicated a role for its cognate G$\beta\gamma$ subunit in the activation of $Ca^{2+}$ channels (21). Additional evidence points to $G\alpha_o$ involvement in signaling from $A_1$-adenosine receptors (22), dopamine D2 receptors (D2R) (23) and $\mu$-opioid signaling (24). A $G\alpha_o$ effector molecule has been reported, GRIN1, which promotes growth cone neurite extension in the mammalian brain (25). The implicated role of $G\alpha_o$ as a mediator and regulator of core neurological and cognitive GPCR-coupled pathways positions $G\alpha_o$ as a prime target for pharmaceutical intervention. A molecular understanding of downstream signaling components is a key step toward identifying potential therapeutic points of drug intervention used

Author contributions: K.C.S., M.A.K., and P.B.S. designed research; K.C.S. and M.A.K. performed research; T.W., C.-K.C., and M.I.S. contributed new reagents/analytic tools; K.C.S., M.A.K., and P.B.S. analyzed data; and K.C.S. and M.I.S. wrote the paper.

The authors declare no conflict of interest.

Data Deposition: The atomic coordinates have been deposited in the Protein Data Bank, www.pdb.org (PDB ID codes 3C7L and 3C7K).

†To whom correspondence may be addressed at: Department of Biology, CB# 3280, 402 Fordham Hall, University of North Carolina, Chapel Hill, NC 27599-3280. E-mail: kslep@bio.unc.edu.

‖Present Address: Institute of Experimental and Clinical Pharmacology and Toxicology, Medical Faculty Mannheim, University of Heidelberg, Maybachstrasse 14, D-68169 Mannheim, Germany.

**To whom correspondence may be addressed at: Division of Biology, California Institute of Technology, Mail Code 147-75, 1200 East California Boulevard, Pasadena, CA 91125. E-mail: simonm@caltech.edu.

††Deceased January 11, 2000.

This article contains supporting information online at www.pnas.org/cgi/content/full/0801569105/DCSupplemental.

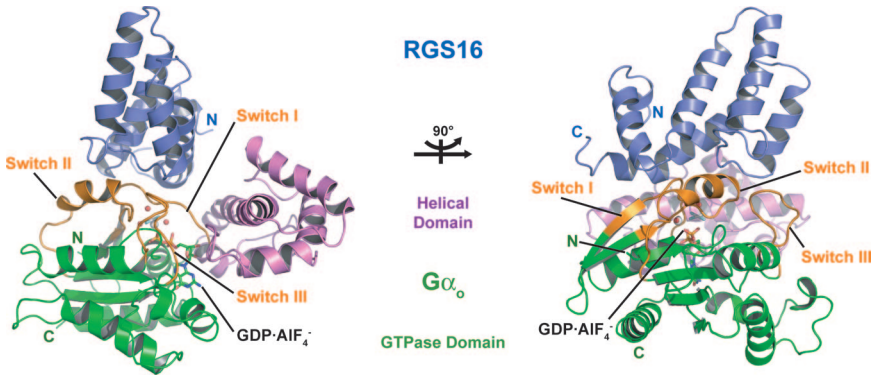


**Fig. 1.** Structure of the $G\alpha_o$·GDP·$AlF_4^-$·RGS16 complex. The $G\alpha_o$·GDP·$AlF_4^-$·RGS16 complex is represented in ribbons format. RGS16 is indicated in gray; $G\alpha_o$ GTPase domain is in green with nucleotide-dependent switch regions highlighted in orange; $G\alpha_o$ helical domain is in purple. Structure at *Right* is rotated 90° about the *y* axis relative to the structure at *Left*.

alone or in combination with GPCR-targeted drugs to minimize side effects (26).

Here, we report the first crystal structure determination of $G\alpha_o$, presented in the transition state of hydrolysis, complexed with the R4 subfamily RGS protein RGS16 (27). $G\alpha_o$ displays a number of unique determinants that likely affords it specificity in receptor, RGS, and effector engagement. We discuss the conserved nature of the RGS GAP mechanism, structural aspects that confer specificity, and the plasticity of the RGS domain required to engage and maintain binding during the transformation of $G\alpha_o$ from the GTP-bound state to the transition state by comparing the $G\alpha_o$·GDP·$AlF_4^-$·RGS16 complex to our independently determined structure of apo-RGS16, also presented here. The Gα–RGS interactions noted in our determination of $G\alpha_o$ complexed to RGS16 dovetails with specificity findings presented in an accompanying article by Soundararajan *et al.* (18), facilitating the first examination of an RGS protein complexed to different Gα subunits.

## Results and Discussion

**Architecture of the $G\alpha_o$·RGS16 Complex.** Mouse $G\alpha_o$ was complexed with mouse RGS16 and purified over gel filtration in the presence of GDP and $AlF_4^-$ to simulate the transition state of GTP hydrolysis. The complex was crystallized in the space group $P3_221$ with two protomers in the asymmetric unit. The structure was determined by molecular replacement, using coordinates from the $G\alpha_{i1}$·GDP·$AlF_4^-$·RGS4 structure (5) and refined to a resolution of 2.9 Å. Crystallographic, phasing, and refinement statistics are presented in supporting information (SI) Table S1. The architecture of the $G\alpha_o$·GDP·$AlF_4^-$·RGS16 complex resembles those observed in $G\alpha_{i1}$·GDP·$AlF_4^-$·RGS4 and $G\alpha_{i1/t}$·GDP·$AlF_4^-$·RGS9 structures (Fig. 1) (5, 7). The RGS domain is positioned almost exclusively on the $G\alpha_o$ switches regions I and II. This is the first structural determination of the $G\alpha_o$ subunit; thus, it cannot be compared with previously solved states of $G\alpha_o$; but, when compared with the solved structures of $G\alpha_{i1}$ and $G\alpha_t$, the $G\alpha_o$ switch conformations most closely resembles that observed in the transition state structures: $G\alpha_{i1}$·GDP·$AlF_4^-$ and $G\alpha_t$·GDP·$AlF_4^-$ (28, 29). $G\alpha_o$ retains the overall domain architecture observed in previously solved Gα structures delineated by a Ras-like GTPase domain encompassing three nucleotide-dependent switch regions and a helical domain, inserted within the Ras-like domain and tethered by two linker regions (28, 30, 31). RGS16, like RGS4 and RGS9, is delineated by nine helices, α1–α9, segregated into two subdomains: one formed by helices α1, α2, α3, α8, and α9 and the other by helices α4, α5, α6, and α7 arranged in an antiparallel four-helix bundle (5, 7). The two subdomains are united by a conserved hydrophobic interface that constitutes the structure's core. RGS16 is a conserved member of the R4 RGS subfamily and retains central conserved elements that define RGS domains except for one component, Thr-158, which replaces the conserved isoleucine or valine found in the equivalent position across all other RGS members (Fig. S1). Thr-158 is buried in the hydrophobic core between the two subdomains. It enhances stabilization through a hydrogen bond to the residue 154 backbone carbonyl and engages the side chain of Phe-93 in a unique geometry independently confirmed by Soundararajan *et al.* (18).

**The RGS16 GAP Mechanism.** The RGS16 RGS domain engages the Gα switch regions via a conserved interface that buttresses their transition state conformation. The interaction is structurally similar to that observed in $G\alpha_{i1}$·RGS4 and $G\alpha_{i1/t}$·RGS9 structures (5, 7). Although the total group of interactions between the RGS domain and the Gα switch regions is not identical between these pairs, key conserved RGS residues are used in identical interactions (Fig. 2*A*). Three critical RGS16 residues are involved near the $G\alpha_o$ active site. RGS16 Asn-90 forms a hydrogen bond to the hydroxyl group of the $G\alpha_o$ Thr-183 side chain. In the $G\alpha_t$·GDP·$AlF_4^-$ structure, this switch I threonine is rotated ≈60° from switch II (29). The orientation observed in the $G\alpha_o$·RGS16 structure allows the Thr-183 side chain to contact switch II residues Lys-211 and Glu-208. This clamps switch I and II together, further stabilizing the transition state conformation from that observed in the $G\alpha_t$·GDP·$AlF_4^-$ structure. A second RGS16 residue, Asp-165, positioned next to switch I, forms a hydrogen bond to the Thr-183 peptide amide. This interaction orients the $G\alpha_o$ Thr-182 backbone carbonyl into the ideal geometry for hydrogen bonding to the nucleophilic water. A third RGS16 residue, Asn-130, is inserted between $G\alpha_o$ residues Lys-181 and Glu-208. Interactions with these two $G\alpha_o$ side chains dictate the orientation of the Asn-130 side chain. In this conformation, the Asn-130 side chain amide forms a hydrogen bond with the $G\alpha_o$ Gln-205 side chain carbonyl. This resolves the torsional ambiguity of the glutamine side chain, orienting it for both stabilization of the nucleophilic water and the planar intermediate. Through these means, RGS16, upon binding $G\alpha_o$ in the activated GTP-bound state, reorients $G\alpha_o$ switches and the residues involved in GTP hydrolysis from their GTP-bound state into their transition state conformation.

Posttranslation modifications have been implicated in increased RGS16 GAP activity. One reported modification is palmitoylation of Cys-98 (Cys-97 in mouse RGS16) (32). Cys-97

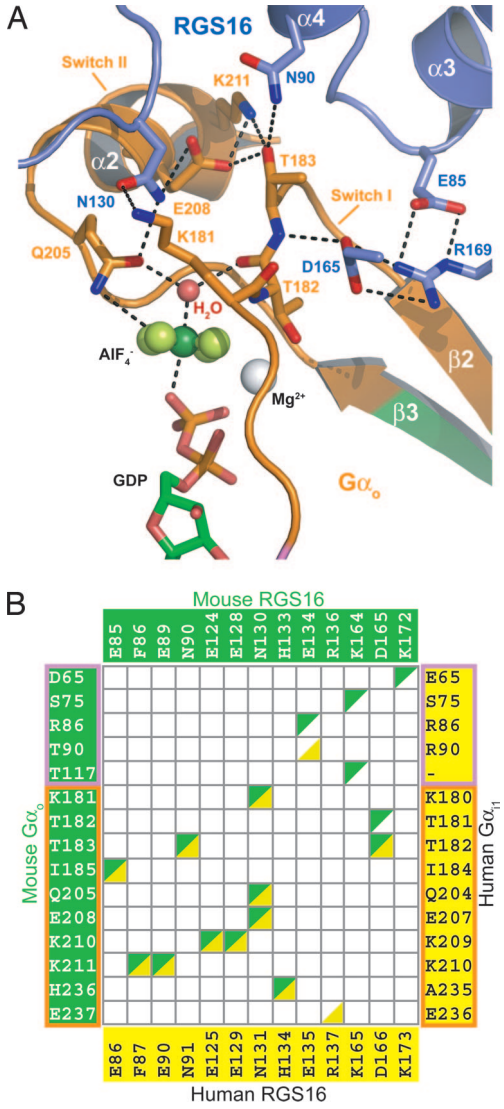


**Fig. 2.** $G\alpha_o$–RGS16 contacts and the RGS domain GAP mechanism. (*A*) Stick-and-ribbons diagram of the $G\alpha_o$ GTP binding pocket occupied by the transition state analog of GTP hydrolysis; GDP·$AlF_4^-$ is shown with $Mg^{2+}$ and the attacking water. $G\alpha_o$ is shown in green and orange (switch regions). RGS16 is shown in purple. RGS16 residues do not contact the GTP or attacking water directly; instead they buttress the endogenous catalytic residues of $G\alpha_o$, stabilizing their conformation in the transition state. (*B*) Comparative <4 Å electrostatic interaction matrix between RGS16 and $G\alpha$ subunits. Electrostatic interactions between mouse $G\alpha_o$ and mouse RGS16 are indicated in green. Electrostatic interactions between human $G\alpha_{i1}$ and human RGS16 are indicated in yellow (PDB ID code 2IK8; see ref. 18). $G\alpha$ switch residues are boxed in orange; helical domain residues are boxed in purple. Interactions that occur in one or both crystallographic protomers are included for both $G\alpha_o$–RGS16 and $G\alpha_{i1}$–RGS16.

projects off helix 4 into the RGS core. A dramatic reorganization of the RGS fold would be required for palmitoylation to occur and any resulting palmitoyl group would project toward the $G\alpha$ subunit. A second modification, phosphorylation of Tyr-168 (Tyr 167 in mouse RGS16) was also reported to increase RGS16 GAP activity (33). The Tyr-167 hydroxyl engages the backbone carbonyl groups of Trp-61 and Arg-62 on helix 1. Tyr-167 phosphorylation would likely precipitate a torsional rotation outwards from its buried position. No apparent contacts between phospho-Tyr-167 and a $G\alpha$ subunit would be predicted, but allosteric modulation of RGS16 GAP activity may result.

**$G\alpha$–RGS Specificity Determinants.** Interactions between the RGS domains and $G\alpha$ subunits determined to date are centered primarily on $G\alpha$ switch regions I and II. Residues in switches I and II that contribute to RGS binding are nearly invariant across $G\alpha$ subunits and do not vary at all across $G\alpha_i$ members $G\alpha_o$, $G\alpha_{i1}$, $G\alpha_{i2}$, $G\alpha_{i3}$, and $G\alpha_t$ (Fig. S2). Outside the $G\alpha_i$ family, RGS specificity is likely to be modulated by the substitution of a lysine at position 181 (relative to $G\alpha_o$) with either a proline or alanine as found in $G\alpha_q$ and $G\alpha_{12/13}$ family members or a leucine as found in the RGS-GAP incompetent family $G\alpha_s$. RGS–$G\alpha$ interactions, however, are not limited exclusively to the nucleotide-dependent switch regions, but may also involve electrostatic interactions with components of the helical domain (Fig. 2*B* and Fig. S2) (7). A higher degree of variation, both within the composition of the $G\alpha$ helical domain and the RGS residues that contact it, provides a platform for specificity proximal to, but independent of, the nucleotide-dependent switch regions.

$G\alpha$–RGS complex structures determined to date have all used different $G\alpha$ subunits and different RGS members. In an accompanying article by Soundararajan *et al.* (18), the human cognate pair $G\alpha_{i1}$·RGS16 is presented, enabling us to directly compare the interactions between $G\alpha_i$ family members ($G\alpha_{i1}$ and $G\alpha_o$) bound to the same RGS member. Analysis of contacts between RGS16 and $G\alpha_i$ members shows that a core set of interactions involving 11 pairs of residues is constant for both $G\alpha_{i1}$ and $G\alpha_o$ (Fig. 2*B*). A number of $G\alpha_{i1}$–RGS16 pairs are unique, including interactions formed between Arg-236–Asp-137 and Arg-90–Glu-135. In the latter pair, an arginine, specific to $G\alpha_{i1}$ and $G\alpha_{i3}$, spans the interaction distance that could not be attained by the equivalent $G\alpha_o$ residue, Thr-90. Unique $G\alpha_o$–RGS16 interactions include an interaction with the GTPase domain Thr-182–Asp-165; interactions with the helical domain including αA residues Asp-65–Lys-172, Ser-75–Lys-164, and Arg-86–Glu-134; and an interaction between RGS16 Lys-164 and Thr-117 on the $G\alpha_o$ αB–αC loop. In addition, residues are used in van der Waals contacts between $G\alpha_o$ and RGS16, including $G\alpha_o$ His-236 (an alanine or valine residue in $G\alpha_i$ family counterparts) that contacts the side chain of RGS16 Asp-132 forming a 4 Å electrostatic interaction between its εN group and the Asp-132 δ carbonyl. As discussed below, prime differences between $G\alpha_o$ and $G\alpha_{i1}$ reside in the helical domain, specifically in terms of side chain diversity and the organization of the αB–αC region. The differential set of interactions between RGS16 and $G\alpha_o$ vs. $G\alpha_{i1}$ is reflected in the total area of solvent accessible surface buried upon complex formation. Analysis of the two $G\alpha_{i1}$·RGS16 structure protomers shows each complex burying 738 $Å^2$ and 802 $Å^2$, respectively. In contrast, $G\alpha_o$·RGS16 structure protomers bury 897 $Å^2$ and 873 $Å^2$, respectively, an average of 115 $Å^2$ more than those observed in the $G\alpha_{i1}$·RGS16 structures, the majority of the differential due to RGS domain–$G\alpha_o$ helical domain contacts. The $G\alpha$ helical domain's role in conferring specificity is likely to be one of a number of factors involved. Although binding determinants between the helical domain and the RGS domain α7 and α8 helices have been observed in $G\alpha_{i1}$·RGS4 (5), $G\alpha_{t/i1}$·RGS9 (7), and the $G\alpha_{i3}$·RGS8 and $G\alpha_{i3}$·RGS10 structures (see ref. 18), no contacts were observed between the $G\alpha$ helical domain and the RGS domain in the $G\alpha_{i1}$·RGS1 and $G\alpha_{i1}$·RGS16 structures.

**Conformational Changes in RGS16.** The independently determined structure of RGS16 alone and in complex with $G\alpha_o$ allows analysis of any conformational changes that occur upon binding the $G\alpha_o$ subunit. A least-squares fitting of the two RGS16 structures over the RGS domain shows little variation in the backbone of the segments that contact $G\alpha_o$ (Fig. 3). Minor movement is noted along the backbone at the α7–α8 linker and N-terminal to α6. Examination of the RGS16 backbone outside

BIOCHEMISTRY

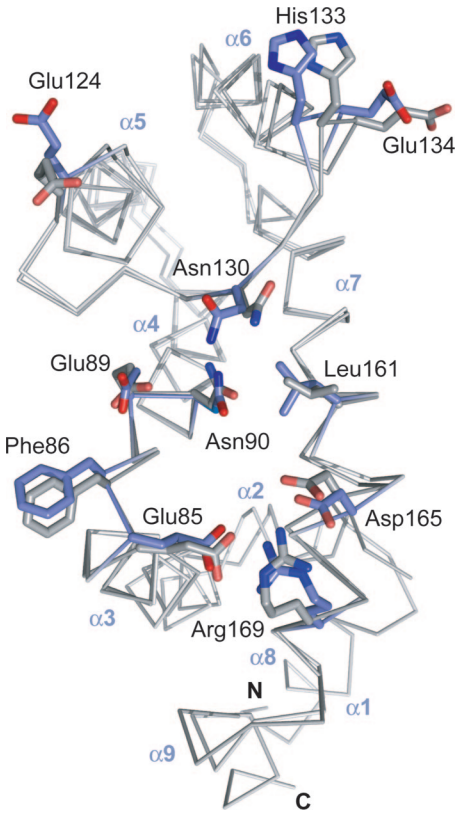


**Fig. 3.** Determinants of RGS16 binding and conformational plasticity. Structural alignment of mouse RGS16 in the free (gray) and $G\alpha_o$-bound (slate) states. The C$\alpha$ trace is presented for both structures, with key residues used in the $G\alpha_o$ interaction represented in stick format. The structural alignment was performed with PyMol.

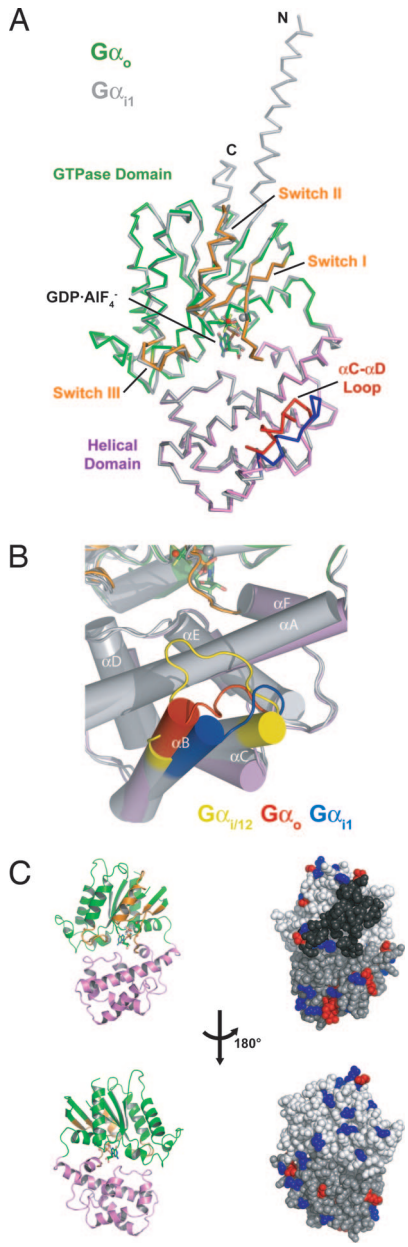


**Fig. 4.** Unique structural determinants in the $G\alpha_o$ helical domain. (*A*) Structural alignment of $G\alpha_o$ and $G\alpha_{i1}$ bound to GDP·$AlF_4^-$, coordinates taken from their respective complex structures with RGS16 and RGS4 [PDB ID code 1AGR (5)] and displayed as a C$\alpha$ trace. $G\alpha_o$ is colored as in Fig. 1*A* except that the divergent $\alpha$B–$\alpha$C loop is shown in red. $G\alpha_{i1}$ is shown in gray except for the comparative $\alpha$B–$\alpha$C loop, which is shown in blue. The structural alignment was performed with PyMol. (*B*) Structural alignment as in *A*, zoomed in on the $\alpha$B–$\alpha$C loop region. $G\alpha_{i/12}$ [PDB ID code 1ZCA (36)] is included, with its respective $\alpha$Bd–$\alpha$C loop region shown in yellow. (*C*) Representation of $G\alpha_o$ in ribbon format (*Left*, colored as in Fig. 1*A*) for orientation and in CPK (*Right*) with the GTPase domain, helical domain, and switch regions colored white, light gray, and dark gray respectively. Residues identical across $G\alpha_{i1\text{-}3}$ and $G\alpha_t$ but not identical in $G\alpha_o$ are mapped in red. Residues identical across $G\alpha_{i1\text{-}3}$ but not identical in $G\alpha_o$ are mapped in blue. Two orientations, related by 180° rotations, are displayed vertically.

the binding region shows a minor reorientation of the N- and C-terminal subdomain formed by $\alpha$1, $\alpha$2, $\alpha$3, $\alpha$8, and $\alpha$9 . In the apo state, this region is pivoted away from the $G\alpha_o$ binding face. This is primarily due to movements in $\alpha$1, $\alpha$2, and $\alpha$9. The N- and C-terminal subdomain is more highly ordered in the apo state with electron density evident for more residues at the N and C termini, potentially indicative of subdomain plasticity when complexed with $G\alpha_o$. RGS16 side chains involved in $G\alpha_o$ switch stabilization undergo a variety of conformational changes. Residues along $\alpha$3 and $\alpha$4, including Glu-85, Phe-86, Glu-89, and Asn-90 undergo modest changes in orientation. In contrast, significant conformational changes are noted for Glu-125 and Asn-130 with large torsional movements ($\approx$120° for Asn-130) to facilitate hydrogen bonding to cognate $G\alpha_o$ residues. The reorientation of Asn-130 is likely coupled to movement of its binding partner, the $G\alpha_o$ residue Gln-205. The corresponding residue in $G\alpha_t$ (Gln-200) was observed to undergo a conformational change between the GTP-bound state and the transition state (29). RGS16 may recognize the key $G\alpha_o$ residue Gln-205 in the active GTP-bound state and dynamically reposition it into the transition state observed in the $G\alpha_o$·GDP·$AlF_4^-$·RGS16 structure. RGS16 side chain movements of note also occur along the $\alpha$6 helix, including His-133 and Glu-134 and along the $\alpha$1 helix, where the Leu-161 side chain rotates toward the binding interface interior, and Asp-165 and Arg-169, linked in a stabilized triad with Glu-85 via the Arg-169 $\delta$-guanido group. This triad undergoes a planar shift of their hydrogen-bonding network facilitated by a rearrangement of Arg-169 into an alternative rotamer via rotations along the C$\alpha$–C$\beta$ and C$\delta$–N$\varepsilon$ bonds. The orientation of this triad mediates the critical interaction between RGS16 Asp-165 and the switch I Thr-183 backbone amide, which in turn positions the Thr-182 backbone carbonyl into optimal geometry for transition state stabilization of the attacking water. The plasticity observed in the RGS16 RGS domain between apo and $G\alpha_o$-complexed states has also been observed in RGS9 and

the independently determined structures of RGS16 in the companion article by Soundararajan *et al.* (18). Domain and side chain rearrangements are a key mechanistic feature of the RGS domain. Although the RGS domain has the highest affinity for Gα in the transition state, it must be able to recognize and bind the activated GTP-bound state and maintain engagement as it reconfigures the complex into the transition state. Subsequently, after releasing Gα-GDP, it must reconfigure, priming itself for subsequent engagement of another activated Gα subunit.

**Structural Features of $G\alpha_o$.** $G\alpha_o$ is a member of the $G\alpha_i$ family and is most closely related to $G\alpha_{i1}$ (34, 35). A comparison of identical vs. nonidentical residues between $G\alpha_o$ and the $G\alpha_i$ family shows that the majority of differences occur in the helical domain, primarily in the αB helix and the αB–αC loop (Fig. 4*C* and Fig. S2). Although no evidence exists that the helical domain serves any function in regard to effector coupling, the differences between $G\alpha_o$ and $G\alpha_{i1}$ raises that possibility. A least-squares fitting of the two molecules reveals a large difference in the αB–αC region. The difference relative to $G\alpha_{i1}$ and $G\alpha_t$ is primarily the result of a proline insertion N-terminal to αC, displacing the αB–αC region ≈6 Å from its comparable position in $G\alpha_{i1}$ and $G\alpha_t$ (Fig. 4 *A* and *B*). Temperature factors for this region of $G\alpha_o$ are slightly elevated above the average main chain temperature factor, likely indicative of mobility within this region. The αB–αC region is a central point of divergence among Gα subunits, particularly for the $G\alpha_{12/13}$ family caused by insertions in the αB–αC loop (Fig. 1*B*). The structures of chimeric $G\alpha_{i/12}$ and $G\alpha_{i/13}$ with intact $G\alpha_{12}$ and $G\alpha_{13}$ helical domains reveal a loop for $G\alpha_{12}$ and an additional helix for $G\alpha_{13}$ that extends from αB and αC toward the switch regions of the GTPase domain (Fig. 4*B*) (36). It is likely that diversity within the αB–αC region is a critical element for GEF, effector, and GAP specificity given its proximity to the nucleotide-dependent switch regions. In strong support for this observation is the finding that GoLoco guanine nucleotide dissociation inhibitor (GDI) motifs target Gα subunits with specificity determinants mediated by the Gα helical domain and the GoLoco C-terminal region. GoLoco motifs from RGS12, RGS14, and AGS3 exert GDI activity on $G\alpha_{i1\text{-}3}$ but not $G\alpha_o$ (37–39). The helical domain's role as a determinant in GDI GoLoco specificity was confirmed through analysis of a $G\alpha_{i1}$–$G\alpha_o$ chimera in which the helical domain of $G\alpha_{i1}$ was replaced with the $G\alpha_o$ helical domain, thus preventing GoLoco-mediated GDI activity on the $G\alpha_{i1}$ GTPase domain (39).

To delineate residues that functionally distinguish $G\alpha_o$ from other $G\alpha_i$ family members, we mapped residues that are identical across $G\alpha_{i1\text{-}3}$ and $G\alpha_t$ but are not identical in $G\alpha_o$ and a second tier of residues that are identical across $G\alpha_{i1\text{-}3}$ but are not identical in $G\alpha_o$ (Figs. 1*B* and 4*C*). The majority of residues unique to $G\alpha_o$ under these criteria map to the helical domain along the αB–αC region. Additional unique residues reside on the opposite face of the Gα subunit, although most also diverge from $G\alpha_{i1\text{-}3}$ in $G\alpha_t$. Although the nucleotide switch regions are highly conserved, a number of unique residues occur in $G\alpha_o$ including Asp-218 in switch II and Gln-233, His-236, Thr-250, and Thr-251 in switch III. The threonine residues on switch III reside proximal to RGS16, implicating them as key nucleotide-dependent determinants for effector–GAP coupling. His-236 of switch III (alanine or valine in $G\alpha_i$ family counterparts) engages RGS16 as mentioned above, contributing van der Waals contacts and electrostatic interactions with RGS16 Asp-132. Gln-233 is buried between the GTPase domain and the helical domain. Asp-218 of switch II (a glycine in $G\alpha_i$ family counterparts) is solvent exposed, and, although distal to the RGS domain (14 Å separation), it may also contribute to nucleotide-dependent effector–GAP coupling determinants.

## Conclusion

The heterotrimeric G protein α subunit is a molecular switch efficiently designed to transmit signaling information from upstream receptors to downstream effectors with high fidelity. G protein α subunits must orchestrate a unique signal transduction pathway amidst hundreds of G protein-coupled receptors and scores of downstream effectors. Functionally, this requires the encoding of higher level specificity. The requirements placed on the Gα subunit include time-dependent activation (endogenous GTPase activity), conformational change to regulate binding partners (nucleotide-dependent switch regions), and binding specificity (unique structural determinants). To regulate α subunit activation temporally and spatially, GAP proteins, including members of the RGS family, are used to bind and enhance the α subunit's endogenous GTPase activity. Although RGS proteins quench G protein activity *in vitro*, it is critical at the cellular level to ensure signal transmission to downstream effectors before inactivation. This paradigm is best illustrated in the visual system where effector–GAP coupling between phosphodiesterase γ and RGS9-$G\beta_5$ ensures efficient, temporally regulated $G\alpha_t$-mediated signal transmission. To extend this paradigm to other Gα subunits, specific effector binding determinants proximal to and nonoverlapping with the α subunit's RGS binding domain are critical. As illustrated in our structure of $G\alpha_o$ and by comparison with $G\alpha_i$ and $G\alpha_{12/13}$ family members, the α subunit's helical domain is a key component with all of the requisite features to facilitate specificity in both effector–GAP coupling and receptor-mediated GEF activity.

Highly enriched in the brain, $G\alpha_o$ likely engages a variety of RGS proteins across anatomical regions, each RGS pairing honed to desensitize $G\alpha_o$ on time scales calibrated for specific neuronal and cognitive tasks. RGS16 localization is specific for the principal relay and midline/intralaminar thalamic nuclei and hypothalamic suprachiasmatic nucleus, sites critical for circadian rhythms and processing sensory input (40). RGS16 and $G\alpha_o$ are uniquely positioned to modulate information dissemination in the brain. Analysis of RGS16 knockout mice or use of inhibitors specifically designed to perturb $G\alpha_o$ or RGS16 function will provide great insight into the neuronal mechanisms the pair govern.

## Materials and Methods: Protein Expression and Purification

Details regarding the expression and purification of $H_6RGS16_{53\text{-}180}$,$G\alpha_o$, complex formation, crystallization, data collection, structure determination, and refinement are in *SI Materials and Methods*.

**ACKNOWLEDGMENTS.** We thank the staff at the Brookhaven National Laboratory (Upton, NY) National Synchrotron Light Source X25 beamline for support, Dr. L. Rice for advice on the Crystallography and NMR System software suite, and Dr. D. Siderovski and A. Kimple for advice on the manuscript. This work was supported in part by a grant from the National Institutes of Health (to P.B.S.) and a Life Sciences Research Foundation/Howard Hughes Medical Institute Fellowship (to M.A.K.).

1. Chan RK, Otte CA (1982) Isolation and genetic analysis of *Saccharomyces cerevisiae* mutants supersensitive to $G_1$ arrest by a factor and alpha factor pheromones. *Mol Cell Biol* 2:11–20.
2. Koelle MR, Horvitz HR (1996) EGL-10 regulates G protein signaling in the *C. elegans* nervous system and shares a conserved domain with many mammalian proteins. *Cell* 84:115–125.
3. Berman DM, Wilkie TM, Gilman AG (1996) GAIP and RGS4 are GTPase-activating proteins for the Gi subfamily of G protein alpha subunits. *Cell* 86:445–452.
4. Berman DM, Kozasa T, Gilman AG (1996) The GTPase-activating protein RGS4 stabilizes the transition state for nucleotide hydrolysis. *J Biol Chem* 271:27209–27212.
5. Tesmer JJ, Berman DM, Gilman AG, Sprang SR (1997) Structure of RGS4 bound to AlF4-activated G(i alpha1): Stabilization of the transition state for GTP hydrolysis. *Cell* 89:251–261.
6. He W, Cowan CW, Wensel TG (1998) RGS9, a GTPase accelerator for phototransduction. *Neuron* 20:95–102.
7. Slep KC, *et al.* (2001) Structural determinants for regulation of phosphodiesterase by a G protein at 2.0 Å. *Nature* 409:1071–1077.
8. Lodowski DT, Pitcher JA, Capel WD, Lefkowitz RJ, Tesmer JJ (2003) Keeping G proteins at bay: A complex between G protein-coupled receptor kinase 2 and Gβγ. *Science* 300:1256–1262.

BIOCHEMISTRY

9. Wilkie TM, Kinch L (2005) New roles for G alpha and RGS proteins: Communication continues despite pulling sisters apart. *Curr Biol* 15:R843–R854.
10. Willars GB (2006) Mammalian RGS proteins: Multifunctional regulators of cellular signalling. *Semin Cell Dev Biol* 17:363–376.
11. Gold SJ, Ni YG, Dohlman HG, Nestler EJ (1997) Regulators of G-protein signaling (RGS) proteins: Region-specific expression of nine subtypes in rat brain. *J Neurosci* 17:8025–8037.
12. Hooks SB, *et al.* (2003) RGS6, RGS7, RGS9, and RGS11 stimulate GTPase activity of Gi family G-proteins with differential selectivity and maximal activity. *J Biol Chem* 278:10087–10093.
13. Snow BE, *et al.* (1998) GTPase activating specificity of RGS12 and binding specificity of an alternatively spliced PDZ (PSD-95/Dlg/ZO-1) domain. *J Biol Chem* 273:17749–17755.
14. Heximer SP, Watson N, Linder ME, Blumer KJ, Hepler JR (1997) RGS2/G0S8 is a selective inhibitor of Gq$\alpha$ function. *Proc Natl Acad Sci USA* 94:14389–14393.
15. Kozasa T, *et al.* (1998) p115 RhoGEF, a GTPase activating protein for G alpha12 and G alpha13. *Science* 280:2109–2111.
16. Wang J, *et al.* (1998) RGSZ1, a Gz-selective RGS protein in brain. Structure, membrane association, regulation by G alpha z phosphorylation, and relationship to a Gz gtpase-activating protein subfamily. *J Biol Chem* 273:26014–26025.
17. Wang Y, *et al.* (2002) Regulator of G protein signaling Z1 (RGSZ1) interacts with G$\alpha$ i subunits and regulates G$\alpha$ i-mediated cell signaling. *J Biol Chem* 277:48325–48332.
18. Soundararajan M, *et al.* (2008) Structural diversity in the RGS domain and its interaction with heterotrimeric G protein $\alpha$-subunits. *Proc Natl Acad Sci USA* 105:●●●–●●●.
19. Chen Z, Wells CD, Sternweis PC, Sprang SR (2001) Structure of the rgRGS domain of p115RhoGEF. *Nat Struct Biol* 8:805–809.
20. Tesmer VM, Kawano T, Shankaranarayanan A, Kozasa T, Tesmer JJ (2005) Snapshot of activated G proteins at the membrane: The G$\alpha$q-GRK2-G$\beta\gamma$ complex. *Science* 310:1686–1690.
21. Valenzuela D, *et al.* (1997) G$\alpha_o$ is necessary for muscarinic regulation of $Ca^{2+}$ channels in mouse heart. *Proc Natl Acad Sci USA* 94:1727–1732.
22. Kudlacek O, *et al.* (2002) Biased inhibition by a suramin analogue of A1-adenosine receptor/G protein coupling in fused receptor/G protein tandems: The A1-adenosine receptor is predominantly coupled to Go$\alpha$ in human brain. *Naunyn Schmiedebergs Arch Pharmacol* 365:8–16.
23. Liu JC, Baker RE, Sun C, Sundmark VC, Elsholtz HP (2002) Activation of Go-coupled dopamine D2 receptors inhibits ERK1/ERK2 in pituitary cells. A key step in the transcriptional suppression of the prolactin gene. *J Biol Chem* 277:35819–35825.
24. Clark MJ, Harrison C, Zhong H, Neubig RR, Traynor JR (2003) Endogenous RGS protein action modulates $\mu$-opioid signaling through G$\alpha_o$. Effects on adenylyl cyclase, extracellular signal-regulated kinases, and intracellular calcium pathways. *J Biol Chem* 278:9418–9425.
25. Nakata H, Kozasa T (2005) Functional characterization of G$\alpha_o$ signaling through G protein-regulated inducer of neurite outgrowth 1. *Mol Pharmacol* 67:695–702.
26. Neubig RR, Siderovski DP (2002) Regulators of G-protein signalling as new central nervous system drug targets. *Nat Rev Drug Discov* 1:187–197.
27. Chen CK, Wieland T, Simon MI (1996) RGS-r, a retinal specific RGS protein, binds an intermediate conformation of transducin and enhances recycling. *Proc Natl Acad Sci USA* 93:12885–12889.
28. Coleman DE, *et al.* (1994) Structures of active conformations of Gi alpha 1 and the mechanism of GTP hydrolysis. *Science* 265:1405–1412.
29. Sondek J, Lambright DG, Noel JP, Hamm HE, Sigler PB (1994) GTPase mechanism of G proteins from the 1.7-Å crystal structure of transducin alpha-GDP-AIF-4. *Nature* 372:276–279.
30. Noel JP, Hamm HE, Sigler PB (1993) The 2.2 Å crystal structure of transducin-alpha complexed with GTP gamma S. *Nature* 366:654–663.
31. Sunahara RK, Tesmer JJ, Gilman AG , Sprang SR (1997) Crystal structure of the adenylyl cyclase activator Gs$\alpha$. *Science* 278:1943–1947.
32. Osterhout JL, *et al.* (2003) Palmitoylation regulates regulator of G protein signaling (RGS) 16 function. II. Palmitoylation of a cysteine residue in the RGS box is critical for RGS16 GTPase accelerating activity and regulation of Gi-coupled signalling. *J Biol Chem* 278:19309–19316.
33. Derrien A, *et al.* (2003) Src-mediated RGS16 tyrosine phosphorylation promotes RGS16 stability. *J Biol Chem* 278:16107–16116.
34. Chen LT, Gilman AG, Kozasa T (1999) A candidate target for G protein action in brain. *J Biol Chem* 274:26931–26938.
35. McIntire WE, Dingus J, Schey KL, Hildebrandt JD (1998) Characterization of the major bovine brain Go$\alpha$ isoforms. Mapping the structural differences between the $\alpha$ subunit isoforms identifies a variable region of the protein involved in receptor interactions. *J Biol Chem* 273:33135–33141.
36. Kreutz B, *et al.* (2006) A new approach to producing functional G$\alpha$ subunits yields the activated and deactivated structures of G$\alpha$(12/13) proteins. *Biochemistry* 45:167–174.
37. De Vries L, *et al.* (2000) Activator of G protein signaling 3 is a guanine dissociation inhibitor for G$\alpha_i$ subunits. *Proc Natl Acad Sci USA* 97:14364–14369.
38. Kimple RJ, *et al.* (2001) RGS12 and RGS14 GoLoco motifs are G$\alpha_i$ interaction sites with guanine nucleotide dissociation inhibitor activity. *J Biol Chem* 276:29275–29281.
39. Kimple RJ, Kimple ME, Betts L, Sondek J, Siderovski DP (2002) Structural determinants for GoLoco-induced inhibition of nucleotide release by G$\alpha$ subunits. *Nature* 416:878–881.
40. Grafstein-Dunn E, Young KH, Cockett MI, Khawaja XZ (2001) Regional distribution of regulators of G protein signaling (RGS) 1, 2, 13, 14, 16, and GAIP messenger ribonucleic acids by *in situ* hybridization in rat brain. *Brain Res Mol Brain Res* 88:113–123.